ELSEVIER

Nuclear Instruments and Methods in Physics Research A 483 (2002) 482–487

NUCLEAR INSTRUMENTS & METHODS IN PHYSICS RESEARCH Section A

www.elsevier.com/locate/nima

Anomalous free electron laser interaction

M. Einat, E. Jerby*, A. Kesar

Faculty of Engineering, Tel Aviv University, University Road, Ramat Aviv 69978, Israel

Abstract

Free electron lasers (FELs) are considered, typically, as fast wave devices. The *normal* FEL interaction satisfies the tuning condition $\omega \cong (k_z + k_W)V_z$, where ω and k_z are the em-wave angular frequency and longitudinal wave number, respectively, V_z is the electron axial speed, and k_W is the wiggler periodicity. This paper presents an *anomalous* FEL interaction, which may occur in slow-wave FELs (i.e. loaded by dielectric or periodic structures). The anomalous FEL effect presented here satisfies the tuning condition $\omega \cong (k_z - k_W)V_z$, and it resembles the anomalous effect in slow-wave cyclotron resonance masers. A necessary condition for the anomalous interaction is $\omega/k_z < V_z$ (i.e., the em-wave phase velocity should be slower than the electron beam). The paper presents a preliminary experimental result demonstrating the anomalous FEL effect in a stripline dielectric-loaded FEL experiment. A linear Pierce equation is applied to describe both the anomalous and normal FELs in the same framework. The paper is concluded with a conceptual discussion.

PACS: 41.60 Cr

Keywords: Free electron laser

1. Introduction

Free electron lasers (FELs) and cyclotron resonance masers (CRMs) can be regarded in common as related devices. Both FELs and CRMs are based on similar interactions between electromagnetic waves and electron beams in wiggling or cycling motions, respectively. Both interactions satisfy the unified synchronism condition

$$\omega = \omega_e + k_z V_{ez} \tag{1}$$

where ω and k_z are the wave-angular frequency and axial wave number, respectively, and $\omega_e = k_e V_{ez}$ is the electron motion frequency where V_{ez} is the axial electron velocity component, and k_e is its corresponding spatial frequency. In FELs, $k_e = k_W$ is the wiggler periodicity, whereas in CRMs $\omega_e = \omega_c$ is the cyclotron frequency.

FELs and CRMs in hollow waveguides are known, typically, as *fast-wave* devices. Their em-wave axial phase-velocity is larger than, or equal to, the speed of light, $V_{ph} = \omega/k_z \geqslant c$. However, beside the common fast-wave mainstream, both FEL and CRM interactions have been investigated also in *slow-wave* structures (dielectric or periodically loaded waveguides) in which $V_{ez} < V_{ph} < c$. Refs. [1–14] and [15–22] represent a two-decade study of slow-wave CRMs and FELs, respectively.

The *anomalous* Doppler effect was proposed and studied in the context of slow-wave CRMs [1,3,4,13,14]. The effect occurs when the em wave

*Corresponding author. Fax: +972-3-640-8048.
E-mail address: jerby@eng.tau.ac.il (E. Jerby).

0168-9002/02/$ - see front matter
PII: S0168-9002(02)00366-2

is slower than the electron beam, $V_{ph} < V_{ez}$, hence the Doppler shift is larger than the em-wave frequency, $k_z V_{ez} > \omega$. Consequently, the synchronism (1) is possible only with a *negative* electron motion frequency,

$$\omega = -\omega_e + k_z V_{ez}. \quad (2)$$

Generic tuning diagrams shown in Figs. 1a and b for the normal and anomalous interactions are illustrations of Eqs. (1) and (2), respectively. The diagrams show on a $\omega - k_z$ map the em-wave dispersion line (in a V_{ph} angle) and the electron-beam line (in a V_{ez} angle). In Fig. 1a, the points A and B denote normal interactions with forward and backward waves, respectively. The Doppler shift is positive for a forward wave, and negative for a backward wave. The interaction in the anomalous mode (Fig. 1b) requires a negative electron-motion frequency and is possible only with a forward slow-wave (Point C). The normal forward-wave interaction (Point A in Fig. 1a) is disabled in the anomalous condition. In a planar-wiggler FEL (unlike an ideal helical-wiggler FEL) the interaction with the backward wave mechanism (Point B in Fig. 1b) remains possible as in the normal condition, but with a lower frequency.

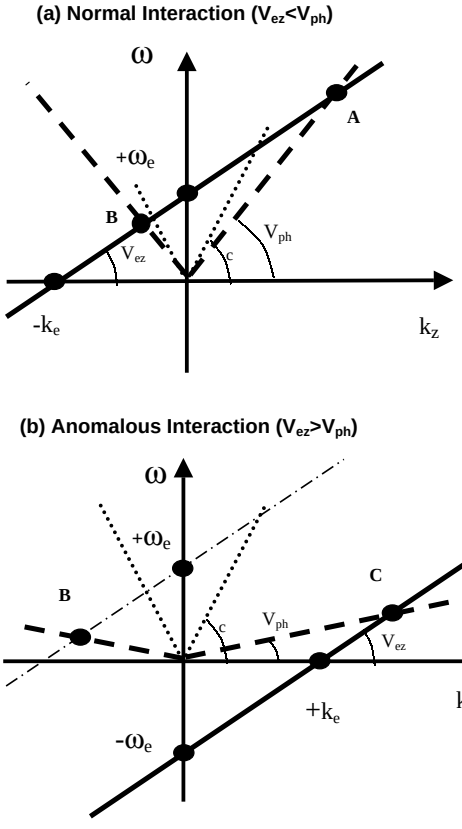

Fig. 1. Generic tuning diagrams for normal (a) and anomalous (b) interactions. For CRMs, ω_e denotes the electron–cyclotron frequency whereas for FELs $\omega_e = k_W V_{ez}$ is the electron wiggling frequency. Points A and B denote the normal forward- and backward-wave interactions, respectively, and Point C denotes the anomalous interaction with a forward wave.

In an analogy to the anomalous CRM [1,3,4,13,14], this paper discusses the feasibility of an *anomalous FEL* operation in an ultra-slow-wave structure, in which the em-wave phase-velocity is slower even than the electron beam itself. The paper presents preliminary experimental observations, which can be attributed to an anomalous FEL effect in a dielectric-loaded stripline FEM. The effect is analyzed by a modified Pierce equation, and its feasibility and applicability are discussed.

2. Experimental setup

An anomalous effect was observed experimentally in the dielectric-loaded stripline FEL. The device, presented earlier in Ref. [20], is shown schematically in Fig. 2. It consists of two copper strips laid along a standard WR90 rectangular

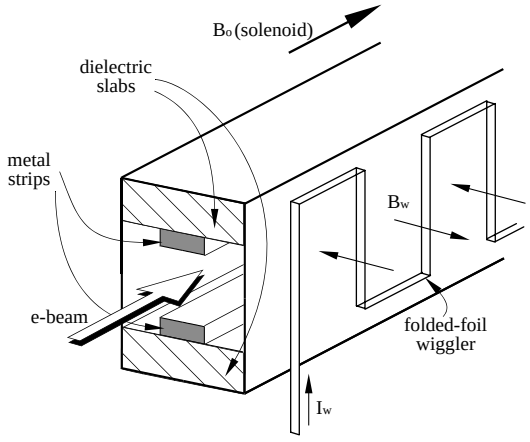

Fig. 2. The FEL experimental scheme

metallic tube. Each copper strip is attached to a dielectric slab along the waveguide wall. The dielectric slabs are made of ceramic (MCT-140 of Trans-Tech Ceramics Inc.) with a dielectric constant of $\varepsilon \approx 140$. The metal strips have both mechanical and electrical functions; they protect the dielectric material from the electron beam and prevent electrical charges and damage to the dielectric slabs. In addition, they support quasi-TEM modes without a cut-off frequency.

The metallic strips stretched parallel to the FEL axis eliminate any axial electromagnetic wave component. Therefore, the longitudinal Cherenkov effect is excluded in this device. The metallic strips ensure that the interaction is indeed a transversal FEL effect.

The double stripline waveguide supports even and odd quasi-TEM modes. Each mode has a different transverse field profile [20], and it propagates in a different phase velocity according to its specific effective dielectric constant ($\varepsilon_{\text{eff}} \approx 8$ for the odd mode, and $\varepsilon_{\text{eff}} \approx 140$ for the even mode).

The dielectric-loaded waveguide (Fig. 2) is installed in our low-voltage FEM/CRM setup [12,14,20,22,23], which consists of a thermionic Pierce electron gun, a WR90 waveguide, a solenoid, and a planar coaxially-fed folded-foil wiggler [24]. The ~ 12 keV electron beams is dumped at the exit of the interaction region onto a collector, which is also used to measure the electron current. Three synchronized pulsers generate the solenoid, the e-gun, and the wiggler pulses, as described in Ref. [12]. The solenoid position can be varied with respect to the device axis, in order to change the electron beam position and to excite different transverse modes.

The FEL oscillator cavity is terminated at both ends by mirrors with holes at the centers for the entrance and exit of the electron beam. A small probe placed in the cavity couples -25 db of the inside radiation power to the output connector. The sampled RF power is attenuated and split into two parallel band-pass filters (BPFs). Oscilloscopes trace the detected outputs of the filters. This diagnostic setup measures the spectral evolution of the oscillator radiation simultaneously with the e-beam voltage.

3. Preliminary results

Figs. 3a and b represent two types of experimental results observed in the setup described above. Each figure shows the electron-gun voltage sweep (i.e. the electron energy variation) at the leading edge of the pulse, and the microwave output signals measured simultaneously during the voltage sweep in three parallel channels. One is a direct detection of the output signal with no filter, and the other two channels include band-pass filters of 2.8–3.1 GHz and 4.5–5.7 GHz noted below as the *lower* and *higher* frequency ranges, respectively.

Fig. 3a shows for instance a normal FEL oscillator behavior in which (as can be seen in Fig. 1a) a decrease in the electron energy, and consequently in their axial velocity, causes a

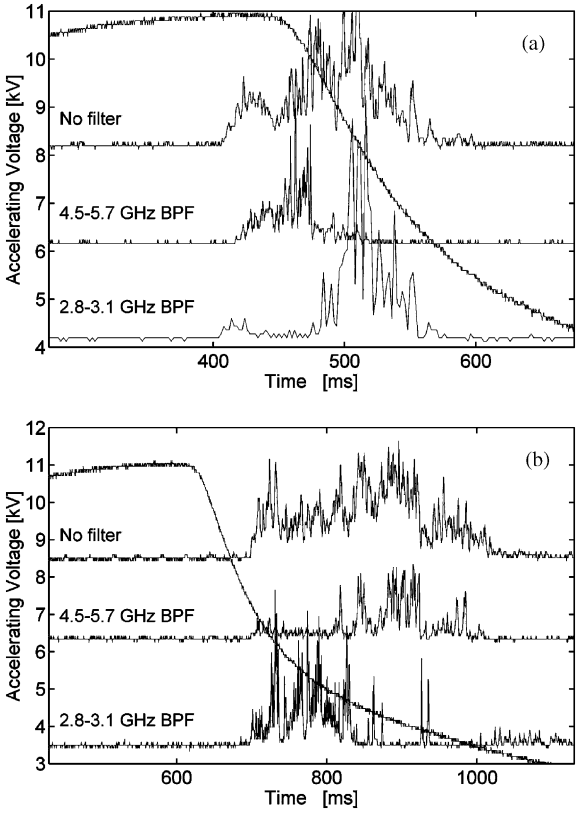

Fig. 3. Experimental results showing the radiation detected output through band-pass filters with respect to the electron accelerating voltage, in normal (a) and anomalous (b) modes.

corresponding decrease in the FEL oscillation frequency. In this example, the higher frequency (~ 5 GHz) is excited at ~ 10 kV, whereas the lower frequency (~ 3 GHz) appears later at a lower voltage (~ 8 kV). Similar results [20] obtained with an electron beam on-axis are attributed to the normal FEL interaction.

Occasionally, when the electron beam is tilted off-axis by the solenoid, an opposite effect occurred, namely the lower frequency appears in a higher voltage than the higher frequency. Fig. 3b shows an example in which the lower frequency (~ 3 GHz) is associated with the higher energy (~ 6 kV) whereas the higher frequency (~ 5 GHz) appears later at 4 kV. Such an opposite tendency of the em-wave frequency and the electron velocity does not characterize a normal FEL synchronism.

The effect observed in Fig. 3b provides a clue to the possibility of an anomalous-Doppler effect in slow-wave FELs. Fig. 1b shows how a decrease in the axial electron velocity is associated with an increase in the oscillation frequency (the intersection point C gets higher). Hence, the anomalous-Doppler effect known in CRMs may explain a similar effect in a slow-wave FEL as well. It should be noted, however, that the same opposite tendency might exist also in a backward-wave CRM (point B in Fig. 1a). This possibility is excluded here by parametric considerations, but it should be taken into account in future studies.

4. Linear theory

A 1D FEL fluid model is modified in this section to include the anomalous-Doppler effect. Assuming a single-mode em-wave polarized in the $\hat{y}$ direction,

$$E_y = A(z)\phi(x)E_0 e^{j(\omega t - k_z z)} \tag{3}$$

where $A(z)$ is the normalized wave amplitude ($A(z=0)=1$), varying slowly along the $\hat{z}$-axis due to the FEL interaction, $\phi(x)$ is the transverse profile of the em-mode, E_0 is its electric field, and ω and k_z are its angular frequency and longitudinal wave number, respectively. The waveguide dispersion relation determines the phase velocity as follows:

$$V_{\rm ph} = \frac{\omega}{k_z} = \frac{c}{\sqrt{\varepsilon_{\rm eff}}} \tag{4}$$

where $\varepsilon_{\rm eff}$ is the effective dielectric factor of the transversely non-uniform waveguide. The electron beam velocity along the planar wiggler (neglecting the solenoid effect) is given by

$$\vec{V} \cong \hat{z}V_{\rm ez} + \hat{y}V_{\rm W}\cos k_{\rm W} z \tag{5}$$

where $V_{\rm W}$ is the transverse amplitude of the electron wiggling velocity.Fast-wave FELs operate at $V_{\rm ph} > c$, whereas the slow-wave FELs satisfies $V_{\rm ph} < c$. The latter, however, can be divided to two different regimes. One is $V_{\rm ez} < V_{\rm ph} < c$ for "ordinary" slow-wave FELs, and the other is $V_{\rm ph} < V_{\rm ez}$ for the "ultra-slow" FEL in which the anomalous behavior is expected. The model studied in this section is applicable for these three regimes, i.e. fast, slow, and ultra-slow FELs.

A straightforward algebraic derivation leads to the FEL linear gain-dispersion relation in the unified Pierce-equation form [25],

$$\bar{A}(s) \cong \frac{[s + j\theta^{(\mp 1)}]^2}{s[s + j\theta^{(\mp 1)}]^2 + j\kappa\theta_p^2} \tag{6}$$

where the tuning parameter is given by

$$\theta^{(\mp 1)} \equiv \frac{\omega}{V_{\rm ez}} - k_z \mp k_{\rm W} \tag{7}$$

for normal ($\theta^{(-1)}$) and anomalous ($\theta^{(+1)}$) FEL regimes. The coupling parameter is

$$\kappa = \frac{1}{8}\frac{\omega}{V_{\rm ez}} F_{\rm f}\left(\frac{V_{\rm W}}{c}\right)^2$$

and the space charge parameter is $\theta_{\rm p} = \omega_{\rm p}/V_{\rm ez}$ where $\omega_{\rm p} = \sqrt{e\rho_0/m\varepsilon_0}$ is the space-charge angular frequency (ρ_0 is the e beam charge density).

Eq. (6) is applied to calculate the single-pass gain for the experimental parameters presented above. The numerical results are shown in Figs. 4a and b for the normal and anomalous FEL interactions with odd and even waveguide modes, respectively. The anomalous gain curve, shown in Fig. 4b, has an opposite S shape orientation to the normal curve shown in Fig. 4a. The gain in the anomalous FEL interaction attains its maximal

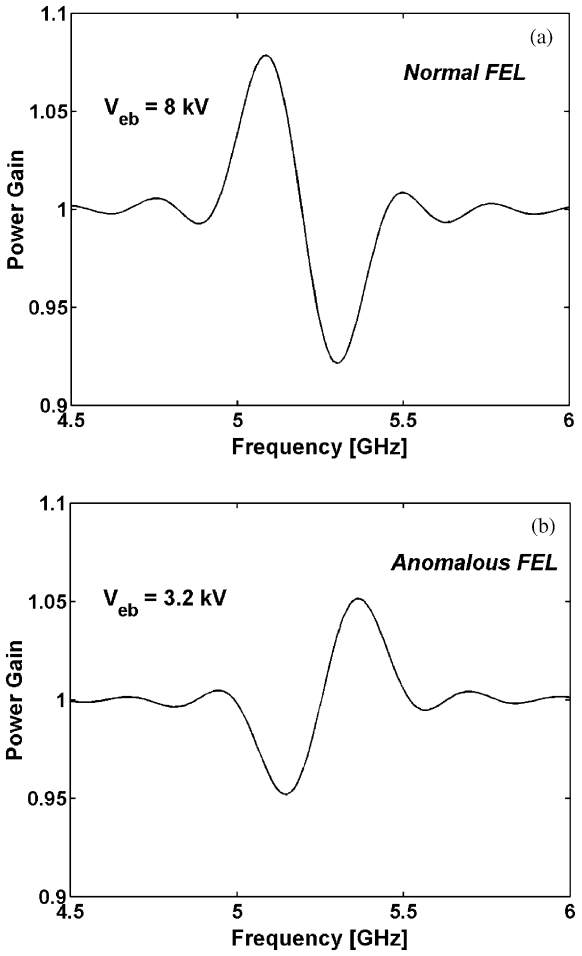

Fig. 4. Numerical results of the power gain with respect to the operating frequency in normal (a) and anomalous (b) modes.

value at a slightly higher frequency than the perfect synchronism point ($\theta = 0$).

The tuning condition for $\theta^{(+1)}$, as well as Eq. (2), including Eq. (4) results in the tuning relation for the anomalous FEL interaction

$$f = \frac{V_{ez}/\lambda_W}{\sqrt{\varepsilon_{eff}}V_{ez}/c - 1} \tag{8}$$

where $\sqrt{\varepsilon_{eff}}V_{ez}/c > 1$. This tuning condition is reversed in the normal interaction. The tuning curves for the normal and anomalous FEL modes observed in this experiment are computed by Eq. (6) as maximum-gain loci on a frequency-voltage map shown in Fig. 5. The dots present

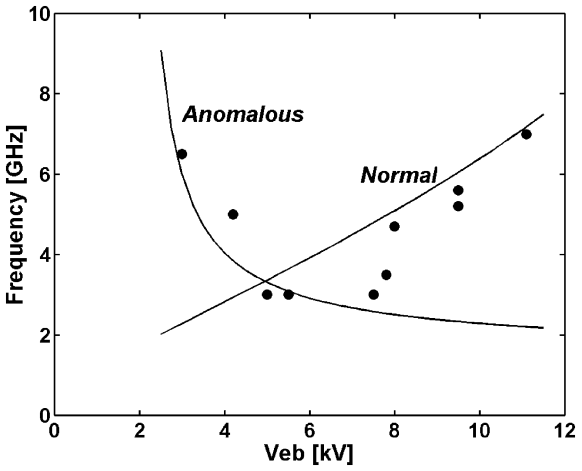

Fig. 5. Tuning curves computed by Eq. (6) as maximum gain loci on a frequency-voltage map for the normal and anomalous FEL experimental parameters. The experimental measurements are indicated by dots.

experimental results. The tendency of the anomalous FEL frequency to grow in low voltages is clearly seen, in agreement with the experimental results.

5. Discussion

The anomalous FEL phenomenon is proposed in this paper on the basis of a preliminary experiment supported by a simple linear FEL model. Further studies are needed to extend the experimental data and to verify its agreement with more detailed theoretical models. Possible interference of backward-wave CRM interactions should be completely eliminated in future anomalous FEL experiments.

The advantages of the slow-wave FEL interaction compared to the fast-wave device are the reduced electron energy for the same frequency (see Figs. 3a and b), and the wider spectral bandwidth. For a planar-wiggler FEL, the dielectric-loaded stripline structure is convenient for impedance matching and coupling at both input and output ports. For a circularly polarized helical-wiggler FEL (unlike the planar-wiggler FEL presented in this study), the anomalous conditions may also eliminate the backward-wave

interaction (Point B in Fig. 1) and its consequent absolute instabilities and spurious oscillations.

The difficulties in using slow-wave structures (dielectric or periodic) stem from the vicinity between the structure and the electron beam, which may cause charging effects and, possibly, damage to the structure. The electron beam current and consequently the amplified microwave power might be limited by this difficulty. This can be overcome by new arrangements of multi-beam anomalous-FEL amplifiers in multi-channel arrays, as proposed for CRMs in Ref. [26].

References

[1] B.I. Ivanov, D.V. Gorozhanin, V.A. Miroshnichenko, Observation of amplification by the anomalous Doppler effect, Pis'ma Zh. Tekh. Fiz. 5 (1979) 1112 [Sov. Tech. Phys. Lett. 5 (1979) 464].

[2] H. Guo, L. Chen, H. Keren, J.L. Hirshfield, S.Y. Park, K.R. Chu, Measurements of gain for slow cyclotron waves on an annular electron beam, Phys. Rev. Lett. 49 (1982) 730.

[3] S.Y. Galuzo, V.L. Slepkov, V.A. Pletyushkin, Relativistic cyclotron accelerator exploiting the anomalous Doppler effect, Zh.Tekh, Fiz. 52 (1982) 1681 [translated from Sov. Phys. Tech. Phys. 27(8) (1982) 1030].

[4] A.N. Didenko, A.R. Borisov, G.P. Fomenko, A. S., Y.G. Shtein, Cyclotron maser using the anomalous Doppler effect, Pis'ma Zh. Tekh. Fiz. 9 (1983) 1331 [translated from Sov. Tech. Phys. Lett. 9 (1983) 572].

[5] T.H. Kho, A.T. Lin, Slow-wave electron cyclotron maser, Phys. Rev. A 38 (1988) 2883.

[6] A.K. Ganguly, S. Ahn, Nonlinear theory of the slow-wave cyclotron amplifier, Phys. Rev. A 42 (1990) 3544.

[7] C.T. Iatrou, J.L. Vomvoridis, Microwave excitation and amplification using cyclotron interaction with an axial electron velocity beam, Int. J. Electron. 71 (1991) 493.

[8] K.C. Leou, D.B. McDermott, N.C. Luhman Jr., Dielectric-loaded wideband Gyro-TWT, IEEE Trans. Plasma Sci. 20 (1992) 188.

[9] Y.Z. Yin, The cyclotron autoresonance maser with a large-orbit electron ring in a dielectric-loaded waveguide, Int. J. Infrared Millimeter Waves 14 (1993) 1587.

[10] E. Jerby, G. Bekefi, Cyclotron maser experiments in a periodic waveguide, Phys. Rev. E 48 (1993) 4637.

[11] E. Jerby, Linear analysis of periodic-waveguide cyclotron maser interaction, Phys. Rev. E 49 (1994) 4487.

[12] E. Jerby, A. Shahadi, V. Grinberg, V. Dikhtiar, M. Sheinin, E. Agmon, H. Golombek, V. Trebich, M. Bensal, G. Bekefi, Cyclotron maser oscillator experiments in a periodically loaded waveguide, IEEE J. Quantum Electron. 31 (1995) 970.

[13] M. Korol, E. Jerby, Quasi-anomalous Doppler effect in a periodic waveguide cyclotron maser, Nucl. Instr. and Meth. A 375 (1996) 222.

[14] M. Einat, E. Jerby, Anomalous and normal Doppler effects in a dielectric-loaded stripline cyclotron resonance masers, Phys. Rev. E 56 (1997) 5996.

[15] M. Ozcan, R.H. Pantell, J. Feinstein, A.H. Ho, Gas-loaded free-electron laser experiments on the Stanford superconducting accelerator, IEEE J. Quantum Electron. 27 (1991) 171.

[16] E. Jerby, Traveling-wave free-electron laser, Phys. Rev. A 44 (1991) 703.

[17] Ling Gen-shen, Liu Yong-gui, Hybrid mode analysis of a slow-wave free-electron laser with a rectangular guide loaded with two slabs of dielectric, Phys. Rev. E 50 (1994) 4262.

[18] G. Mishra, K.P. Maheshwari, G. Praburam, A slow wave free-electron laser in a longitudinal wiggler field, IEEE Trans. Plasma Sci. 21 (1994) 181.

[19] T. Shiozawa, M. Mikawa, Efficiency enhancement in a dielectric-loaded Raman-type free-electron laser, IEEE J. Quantum Electron. 30 (1994) 2676.

[20] M. Einat, E. Jerby, A. Shahadi, Dielectric-loaded free-electron maser in stripline structure, Nucl. Instr. Meth. A 375 (1996) 21.

[21] D.E. Pershing, R.H. Jackson, H.P. Freund, M. Blank, K. Nguyen, J.M. Taccetti, Design of a slow-wave ubitron, Nucl. Instr. Meth. A 375 (1996) 230.

[22] R. Drori, E. Jerby, Tunable fluid-loaded free-electron-laser in the low electron-energy and long-wavelength extreme, Phys. Rev. E 59 (1999) 3588.

[23] R. Drori, E. Jerby, A. Shahadi, Free-electron maser oscillator experiment in the UHF regime, Nucl. Instr. and Meth. A 358 (1995) 151.

[24] A. Sneh, E. Jerby, Coaxially fed folded foil electromagnet wiggler, Nucl. Instr. and Meth. A 285 (1989) 294.

[25] A. Gover, P. Sprangle, A unified theory of magnetic bremsstrahlung, electromagnetic bremsstrahlung, Compton–Raman scattering, and Cherenkov–Smith–Purcell free-electron lasers, IEEE J. Quantum Electron. 17 (1981) 1196.

[26] E. Jerby, A. Kesar, M. Korol, L. Lei, V. Dikhtyar, Cyclotron resonance maser array, IEEE Trans. Plasma Sci. 27 (1999) 445.